Ceramics International (xxxx) xxxx–xxxx

Contents lists available at ScienceDirect

Ceramics International

journal homepage: www.elsevier.com/locate/ceramint

Role of nitrogen-related complex in stabilizing ferromagnetic ordering in a rare-earth and nitrogen codoped ZnO

Jinhuan Jia[a], Yongfeng Li[a,b,*], Bin Yao[a,b], Zhanhui Ding[a], Ruijian Liu[a], Rui Deng[c], Ligong Zhang[d], Haifeng Zhao[d], Lei Liu[d]

[a] State Key Lab of Superhard Material and College of Physics, Jilin University, Changchun 130012, China
[b] Key Laboratory of Physics and Technology for Advanced Batteries (Ministry of Education), College of Physics, Jilin University, Changchun 130012, China
[c] School of Materials Science and Engineering, Changchun University of Science and Technology, Changchun 130022, China
[d] State Key Lab of Excited State Processes, Changchun Institute of Optics, Fine Mechanics and Physics, Chinese Academy of Sciences, Changchun 130033, China

ARTICLE INFO

Keywords:
ZnO
Diluted magnetic semiconductor
Ferromagnetism
Magnetron sputtering
First-principle calculation

ABSTRACT

We report the ferromagnetic enhancement in a rare-earth and nitrogen co-doped ZnO thin film. To reveal the origin of ferromagnetism, we perform a comparative study on undoped, Nd-doped, N-doped and (Nd, N)-codoped ZnO thin films by combining experiments with first-principles calculations. Compared with the Nd-doped ZnO, the N incorporation into the Nd-doped ZnO to form $2Nd_{Zn}$-N_O complex leads to the more stable ferromagnetic coupling between two Nd atoms, which is well supported by first-principles calculations. Our results suggest that the electronic structure alteration via codoping engineering plays a critical role in stabilizing the ferromagnetic orderings.

1. Introduction

Over the past two decades, diluted magnetic semiconductors (DMSs) have attracted much attention due to their potential applications in spin electronics and magnetic devices [1,2]. Compared with the conventional semiconductor, cations in DMSs are partly substituted by magnetic ions so that DMSs are expected to have high Curie temperature (T_C) exceeding room temperature [3,4] and utilize both charge and spin degrees of freedom [1,5–7]. The novel behavior of DMSs leads to the potential applications in the new emerging fields of semiconductor spintronic devices, spin polarized light emitting diodes, photovoltaics and sensors [8–13]. Among the various material candidates as DMSs [14,15], most of researches have been mainly focused on ZnO owing to the theoretically predicted room temperature ferromagnetism [16–20]. Furthermore, ZnO has excellent properties, such as a direct wide-bandgap of 3.37 eV and a large exciton binding energy of 60 meV at room temperature [21–23]. Although room temperature ferromagnetism in transition metals (TMs) doped ZnO has been reported, the magnetism is often weak [24]. Compared with TMs, rare-earth (RE) metals with open f shells, often offer larger magnetic moment. Indeed, both theoretical and experiments studies revealed that Gd-doped GaN exhibits a colossal magnetic moment [25,26]. Therefore, it remains an open question whether RE doping can induce strong room temperature ferromagnetism in ZnO. However, up to now, RE elements have been much less pursued as dopants in ZnO that shows room temperature ferromagnetism, even if recent theoretical and experiments studies have indicated that RE-doped (RE=Gd, Nd) doped ZnO films only show paramagnetic behavior or very weak ferromagnetism at room temperature [27–30]. In the recent years, the codoping approach, especially donor-acceptor cooping, has been intensively studied due to the possibility to tailor the position and occupancy of the Fermi energy of doped DMSs [31]. For instance, Wang *et al.* observed room temperature ferromagnetism in the (Mn, N)-codoped ZnO [32]. In our previous work, it was also observed that donor-acceptor complex in SnO_2 induce room temperature ferromagnetism [33]. Therefore, codoping is likely to be a potential approach to enhance the ferromagnetism of ZnO.

In this article, we conducted a comparative study on undoped, Nd-doped, N-doped and (Nd, N)-codoped ZnO via complementary experiments and first-principles calculations based on spin-polarized density functional theory (DFT). In the (Nd, N)-codoped ZnO thin film, we observed ferromagnetic enhancement at room temperature. The first-principles calculations reveal that the N incorporation into the Nd-doped ZnO results in the more stable ferromagnetic ordering between two Nd atoms, which well supports our experimental results.

* Corresponding author at: State Key Lab of Superhard Material and College of Physics, Jilin University, Changchun 130012, China.
E-mail addresses: liyongfeng@jlu.edu.cn (Y. Li), binyao@jlu.edu.cn (B. Yao).

http://dx.doi.org/10.1016/j.ceramint.2017.01.140
Received 12 December 2016; Received in revised form 26 January 2017; Accepted 28 January 2017

2. Experimental and first-principles calculations details

Undoped, Nd-doped, N-doped and (Nd, N)-copded ZnO films were deposited on c-plane sapphire substrates by radio-frequency (RF) magnetron sputtering. The pure and Nd-doped ZnO ceramic targets were sintered by high purity ZnO (99.99%, Alfa Aesar) and the mixture of the ZnO and Nd_2O_3 (99.99%, Alfa Aesar) powder with a mole ratio of 99:1, respectively. The pressure of the growth chamber was evacuated to be 3×10^{-4} Pa before deposition, and then filled with sputtering gas and was kept at 1.0 Pa during depositing process. The pure Ar gas was used as work gas for the undoped and Nd-doped ZnO films, and the mixed gases of Ar and N with a flow ratio of 3:1 for the N-doped and (Nd, N)-codoped ZnO films. All thin films were sputtered for 1 h at deposition temperature of 500 °C.

X-ray diffraction (XRD) was used to determine crystal structures using an X-ray diffractometer with Cu *Kα* radiation (λ=0.15418 nm). Chemical states and compositions were determined using X-ray photoelectron spectroscopy (XPS). The adventitious C 1*s* peak at 284.6 eV was used to calibrate the binding energy. The concentrations of Nd and N for the Nd-doped and N-doped ZnO films were determined to be 2.8 at% and 1.0 at%, as well as 2.6 at% and 1.8 at% for the (Nd, N)-codoped ZnO films, respectively. Magnetization measurements were performed using a superconducting quantum interference device magnetometer (SQUID, Quantum Design, MPMSXL-5). The optical absorption measurements were performed using a UV–vis–near-IR spectrophotometer. The photoluminescence (PL) measurements were performed using a He–Cd laser with a 325-nm line as the excitation source.

In the first-principles calculations based on density functional theory (DFT), we adopted the VASP code with the projector augmented wave (PAW) potentials for the electronic interaction and the generalized gradient approximation (GGA) for the electron exchange and correlation [34–37]. The cutoff energy of 400 eV for the plane-wave basis was used and a 72-atom 3×3×2 supercell with the wurtzite structure was constructed. In the ZnO supercells, we constructed three different configurations for simulating the doped ZnO: (i) Two nearest-neighbor O atoms are substituted by two N atoms to form N_O-N_O configuration; (ii) Two nearest-neighbor Zn atoms are substituted by two Nd atoms to form Nd_{Zn}-Nd_{Zn} configuration; (iii) One O atom between two Nd atoms are substituted by one N atom to form $2Nd_{Zn}$-N_O complex. For the Brillouin-zone integration, a 3×3×3 Monkhorst-Pack k-point mesh was used; a more refined (8×8×8) k-point mesh was used for the density-of-states (DOS) calculations. In the supercell optimization calculations, all the atoms are allowed to relax until the Hellmann-Feynman forces acting on them become less than 0.01 eV/Å.

3. Results and discussion

Fig. 1 shows the XRD patterns of undoped ZnO, Nd-doped ZnO, N-doped ZnO and (Nd, N)-codoped ZnO films grown on *c*-Al_2O_3 substrates. For all the samples, only ZnO (002) diffraction peak is observed, indicating the ZnO films have the wurtzite structure with a preferred orientation and no impurity phase is detected. The enlarged ZnO (002) peaks are shown in the right panel of Fig. 1 for clearly demonstrating the peak positions. The (002) diffraction peaks of the doped ZnO films have a shift towards low diffraction angle with respect to the undoped ZnO films. The ionic radii of the Nd, Zn, N and O are 0.98, 0.74, 1.46 and 1.40 Å determined by Shannon [38]. The larger ionic radius of Nd and N than Zn and O lead to the lattice expansion, resulting in the peak shift towards to low diffraction angle. Therefore, the diffraction peak shifts confirm that the corresponding doping atoms are incorporated into ZnO lattices.

To determine the chemical states of dopants in ZnO, XPS measurements were carried out. Fig. 2(a) shows the XPS spectra of Nd 3*d* in the ZnO:Nd and ZnO:(Nd,N) films. The binding energy values obtained for Nd $3d_{3/2}$ and Nd $3d_{5/2}$ are 998.7 and 982.1 eV, respectively, confirming the trivalent state of Nd in the Nd doped and (Nd, N)-codoped ZnO films [39]. Fig. 2(b) shows the XPS spectra of N 1*s* in the ZnO:N and ZnO:(Nd,N) films. The N 1*s* spectrum displays one peak at 395.8 eV. It should be pointed that the binding energy of N 1*s* state varies from 395 to 408 eV as chemical environment of nitrogen atom changes [40]. The peak at 396 eV is assigned to nitrogen substitution at oxygen site (N_O), acting as acceptor [41].

Fig. 3 shows the optical absorption data of $(\alpha h\nu)^2$ versus $h\nu$, where α is the absorption coefficient and $h\nu$ is the photon energy. Using Tauc rule [42]: $\alpha h\nu \propto (h\nu - E_g)^{1/2}$, the bandgaps of undoped ZnO, N-doped ZnO, Nd-doped ZnO and (Nd, N)-codoped ZnO are 3.29, 3.26, 3.33 and 3.31 eV, respectively. The bandgap of the N-doped ZnO is slightly smaller than the undoped ZnO, which is ascribed to the occurrence of band tail states introduced by N acceptor incorporation. The bandgap of the Nd-doped and (Nd, N)-codoped ZnO is significantly larger than the undoped ZnO, which is due to Burstein-Moss effect [43,44]. It should be noted that the absorption edge of the (Nd, N)-codoped ZnO is smaller than the Nd-doped ZnO. The doped Nd and N atoms act as donors and acceptors in ZnO film, respectively. As a result, a passivated donor-acceptor impurity band can occur in the bandgap when a large

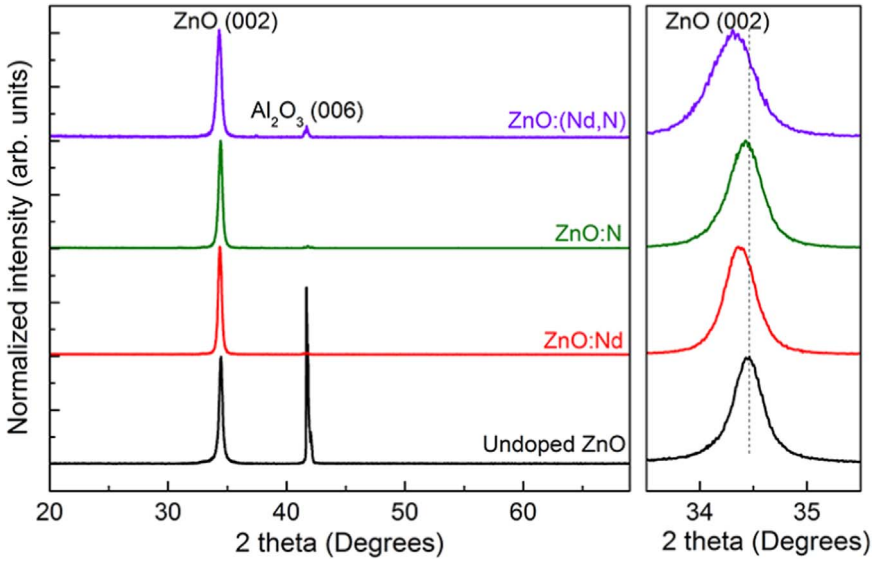

Fig. 1. Normalized XRD patterns of the undoped, Nd-doped, N-doped and Nd-N codoped ZnO thin films. The enlarged ZnO (002) peaks are shown in the right panel.